Journal of Solid State Chemistry 199 (2013) 154–159

Contents lists available at SciVerse ScienceDirect

Journal of Solid State Chemistry

journal homepage: www.elsevier.com/locate/jssc

Crystal structure and oxygen content of the double perovskites $GdBaCo_{2-x}Fe_xO_{6-\delta}$

D.S. Tsvetkov*, I.L. Ivanov, A.Yu. Zuev

Department of Chemistry, Institute of Natural Sciences, Ural Federal University, Lenin Av. 51, 620000 Ekaterinburg, Russia

ARTICLE INFO

Article history:
Received 27 August 2012
Received in revised form
9 November 2012
Accepted 14 December 2012
Available online 27 December 2012

Keywords:
Oxygen content
Double perovskite
Structure transition

ABSTRACT

The iron solubility limit, x, in $GdBaCo_{2-x}Fe_xO_{6-\delta}$ determined by means of X-ray diffraction was found to be close to 0.65 in air. The crystal structure changes of the double perovskites $GdBaCo_{2-x}Fe_xO_{6-\delta}$ ($x=0$–0.6) were studied by means of "in situ" X-ray diffraction in temperature range from 25 to 900 °C in air. The oxygen content, $6-\delta$, was determined for these double perovskites in air as a function of temperature by means of thermogravimetric technique in range $25 \le T$, °C $\le$ 1100. The *Pmmm*-*P4*/*mmm* structure transition was found to occur in $GdBaCo_{2-x}Fe_xO_{6-\delta}$ ($0 \le x \le 0.4$) with increasing temperature. This transition is observed at the same temperature for the compositions with $0 \le x \le 0.1$ while the transition temperature reaches maximum for $x=0.2$ and that decreases linearly with further iron increase. The double perovskite $GdBaCo_{1.4}Fe_{0.6}O_{6-\delta}$ was shown to have the tetragonal *P4*/*mmm* structure at room temperature. The *P4*/*mmm*-*Pmmm* structure transition occurs at temperature as low as 170 °C for this double perovskite while reverse one is already observed at 290 °C in air. The *Pmmm*-*P4*/*mmm* structure transition was found to be strongly related to the oxygen content for the undoped and slightly doped ($x \le 0.2$) double perovskites while there is no such relation for the double perovskites enriched by iron ($x \ge 0.2$).

1. Introduction

Mixed ionic and electronic conducting oxides $AA'Co_2O_5$, where A is a rare earth element (RE), A' – Ba, with double perovskite structure have received great attention in past decade [1–4] due to their unique magnetic and transport properties at relatively low temperatures. In particular, $GdBaCo_2O_{6-\delta}$ was shown to possess sufficiently high oxygen ionic conductivity and oxygen chemical diffusion coefficient at temperatures as low as 400 °C [3]. Double perovskite $GdBaCo_2O_{6-\delta}$ was recently found to exhibit excellent performance as a cathode for IT SOFCs [5–7] and oxygen permeable dense ceramic membrane [6]. However, despite promising cathode behavior of $GdBaCo_2O_{6-\delta}$ some undesirable properties such as high thermal expansion coefficient (TEC) [5] and low temperature phase transition [8] accompanied by significant increase of the lattice volume seriously restrict its commercial application. Doping $GdBaCo_2O_{6-\delta}$ with other 3d-metal seems to be a possible way to solve the aforementioned problems. Indeed substitution of iron for cobalt was recently shown to decrease the TEC value [9] of $GdBaCo_2O_{6-\delta}$.

Tarancón et al. [10] first observed a low temperature transition in the vicinity of 88 °C and the structural transition from orthorhombic *Pmmm* to tetragonal *P4*/*mmm* space group at 476 °C for the double perovskite $GdBaCo_2O_{6-\delta}$ in air atmosphere. Small substitution (10 mol.%) of iron for cobalt was also found [11] to lead to disappearance of low temperature transition and to increase of *Pmmm*–*P4*/*mmm* transition temperature up to 515 °C. The latter was shown [11] to occur due to some oxygen content increase caused by iron doping. Actually the oxygen content reaches the threshold value of 5.47 (corresponding to elimination of oxygen vacancies ordering along *b*-axis) at 475 °C [12] and at 515 °C [11] for $GdBaCo_2O_{6-\delta}$ and $GdBaCo_{1.8}Fe_{0.2}O_{6-\delta}$, respectively, in air.

So far, however, there are no data on a structure of Fe-doped double perovskites $GdBaCo_{2-x}Fe_xO_{6-\delta}$ ($x > 0.2$) depending on temperature. Moreover a solubility limit of iron and value of oxygen content in $GdBaCo_{2-x}Fe_xO_{6-\delta}$ still remain controversial topics [9,13].

Therefore the priority purposes of the present work were (i) to elucidate a solubility limit of iron in the double perovskite $GdBaCo_2O_{6-\delta}$, (ii) to study the crystal structure of the double perovskites $GdBaCo_{2-x}Fe_xO_{6-\delta}$ as a function of temperature in air, (iii) to measure oxygen nonstoichiometry of $GdBaCo_{2-x}Fe_xO_{6-\delta}$ as a function of temperature in air, and (vi) to find a possible relationship between a structure alteration and oxygen content for the double perovskites investigated.

2. Experimental

Powder samples of nominal composition $GdBaCo_{2-x}Fe_xO_{6-\delta}$ ($x=0$–1.0) were prepared by means of glycerol–nitrate method

* Corresponding author. Fax: +7 343 261 5978.
E-mail address: Dmitrii.Tsvetkov@usu.ru (D.S. Tsvetkov).

0022-4596/$ - see front matter © 2012 Elsevier Inc. All rights reserved.
http://dx.doi.org/10.1016/j.jssc.2012.12.013

using Gd_2O_3, $BaCO_3$, Co, $FeC_2O_4{}^*2H_2O$ as starting materials. All materials used had a purity of 99.99%.

Stoichiometric mixture of starting materials was dissolved in concentrated nitric acid (99.99% purity) and required volume of glycerol (99% purity) was added as a complexing agent and a fuel. Glycerol quantity was calculated according to full reduction of corresponding nitrates to molecular nitrogen N_2. As prepared solution was heated continuously at 100 °C until water evaporation and pyrolysis of the dried precursor. The resulting ash was subsequently calcined at 1100 °C for 10 h to get the desired double perovskite powder.

The phase composition of the powder samples prepared accordingly was studied at room temperature by means of X-ray diffraction (XRD) with Equinox 3000 diffractometer (Inel, France) using Cu $K\alpha$ radiation. XRD showed no indication for the presence of a second phase for as prepared compositions with $0 \le x \le 0.6$.

The crystal structure of the double perovskites $GdBaCo_{2-x}Fe_xO_{6-\delta}$ (x=0–0.6) was studied in the temperature range between 25 and 900 °C in air by means of "in situ" XRD with Cu $K\alpha$ radiation using Equinox 3000 diffractometer (Inel, France) equipped with the high temperature camera HTK 16 N (Anton Paar GmbH, Austria).

Oxygen nonstoichiometry, δ, as a function of temperature in air was studied by means of thermogravimetric (TG) technique using a STA409PC (Netzsch, Germany) microbalance. A sample was equilibrated first at the given oxygen partial pressure (pO_2= 0.21 atm) and temperature for 2 h until a sample weight ceases to change. Temperature was then changed in steps within range between 25 and 1150 °C in both decreasing and increasing direction at the same pO_2=0.21 atm and the measurement procedure was repeated until equilibrium state was reached at each step. Absolute value of δ in $GdBaCo_{2-x}Fe_xO_{6-\delta}$ (x=0–0.6) samples was determined by both direct reduction of corresponding double perovskites by hydrogen flux in the TG setup (TG/H_2) and iodometric titration of the samples slowly cooled to room temperature. Both methods are described in detail elsewhere [12].

3. Results and discussion

X-ray diffraction patterns of as prepared and slowly (~100 °C/h) cooled powder samples of nominal composition $GdBaCo_{2-x}Fe_xO_{6-\delta}$ (x=0–1) are given in Fig. 1. This figure obviously shows that the

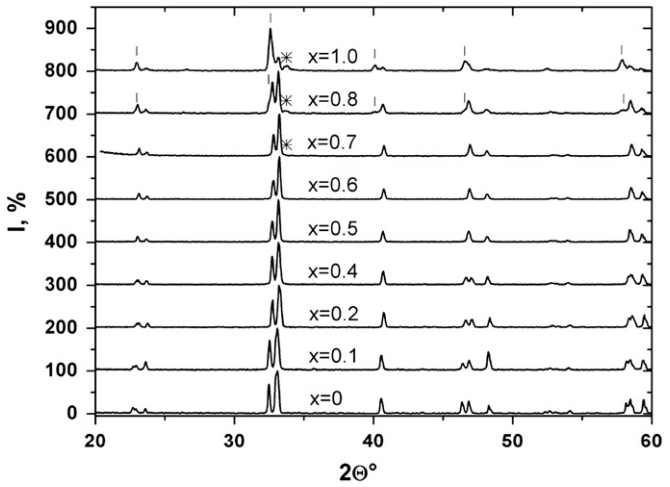

Fig. 1. XRD profiles of slowly (~100 °C/h) cooled double perovskites of nominal compositions $GdBaCo_{2-x}Fe_xO_{6-\delta}$ (x=0–1.0). | – cubic $Ba_{1-y}Gd_yFeO_3$; * – $GdFe_{1-z}Co_zO_3$.

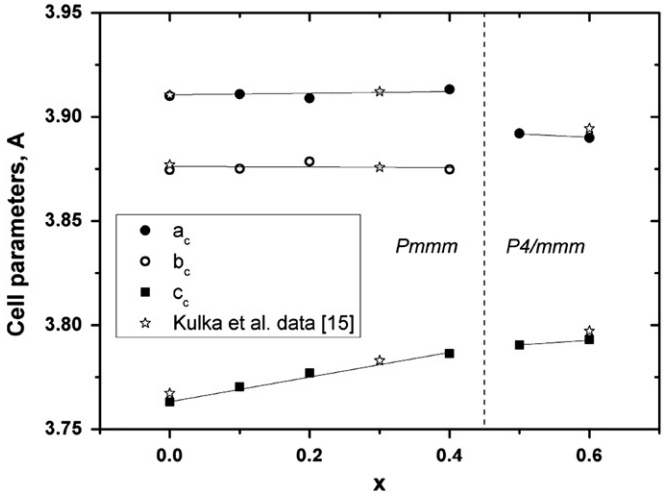

Fig. 2. Lattice parameters of $GdBaCo_{2-x}Fe_xO_{6-\delta}$ (x=0–0.6) as a function of Fe content at room temperature.

double perovskites of compositions x=0–0.6 are single phases whereas the patterns for as prepared samples with $x \ge 0.7$ contain peaks relating to impurities. Perovskite phases $Ba_{1-y}Gd_yFeO_3$ and $GdFe_{1-z}Co_zO_3$ were identified as these impurities. The solubility limit, x_{max}, therefore, lies in the composition range between 0.6 and 0.7. Thus the results obtained on a solubility limit of iron for $GdBaCo_{2-x}Fe_xO_{6-\delta}$ in air do support neither those reported earlier by Kim et al. [9] who found that x_{max}=1.0 nor those of Medvedev et al. [13] who determined x_{max} as high as 1.2.

XRD patterns of the single phases $GdBaCo_{2-x}Fe_xO_{6-\delta}$ with x=0–0.4 were indexed using the orthorhombic *Pmmm* space group (unit cell $a_c \times 2a_c \times 2a_c$, where a_c is the lattice parameter of the cubic cell) whereas indexing of those with higher iron content x=0.5 and 0.6 revealed the presence of the tetragonal phase with *P4/mmm* symmetry. The lattice parameters of $GdBaCo_{2-x}Fe_xO_{6-\delta}$ (x=0–0.6) are given in Fig. 2 as a function of iron content at room temperature in air. It is worth noting that a and b cell parameters of the Fe-doped double perovskites are very close to those of the undoped cobaltite $GdBaCo_2O_{6-\delta}$ in the composition range $0 \le x \le 0.4$. In other words, they do not depend on the iron content whereas c parameter increases with iron substitution. These results seem to be in good agreement with those reported earlier by Thirumurugan et al. [14] and Kulka et al. [15].

It also follows from Fig. 2 that the structure transition from *Pmmm* to *P4/mmm* space group upon substitution of iron for cobalt in $GdBaCo_{2-x}Fe_xO_{6-\delta}$ occurs in vicinity of x=0.45 at room temperature. Kim et al. [9] also observed the *Pmmm-P4/mmm* transition for the double perovskite $GdBaCo_{2-x}Fe_xO_{6-\delta}$ with increasing iron content and supposed that it is caused by simultaneous oxygen content increase up to value of 6 that destroys the oxygen vacancies ordering observed at oxygen content values close to 5.5 [10,11].

X-ray diffraction pattern of $GdBaCo_{1.6}Fe_{0.4}O_{6-\delta}$ sample obtained in the temperature range between 25 and 800 °C in air is shown, as an example, in Fig. 3. As follows the pattern alters significantly with temperature obviously indicating the *Pmmm-P4/mmm* structure transition. Coexistence of *Pmmm* and *P4/mmm* phases is obviously shown in the range $45 \le 2\Theta, ^\circ \le 50$ marked by dashed lines in Fig. 3. Such coexistence was found to take place in the pattern obtained at 445 °C.

Thus the low temperature XRD patterns for the samples with x=0 and 0.4 were indexed using the orthorhombic *Pmmm* space group (unit cell $a_c \times 2a_c \times 2a_c$, where a_c is the lattice parameter of the cubic cell) and high temperature ones – the tetragonal *P4/mmm* one.

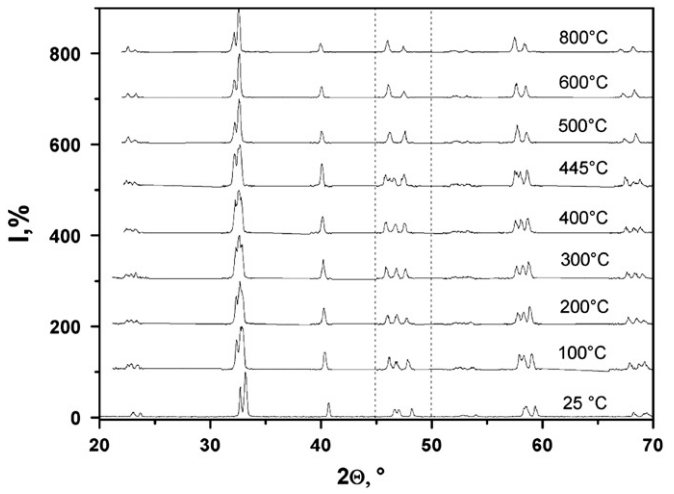

Fig. 3. In situ XRD patterns of $GdBaCo_{1.6}Fe_{0.4}O_{6-\delta}$ in the temperature range between 25 and 800 °C in air.

The lattice parameters of the double perovskites $GdBaCo_{2-x}Fe_xO_{6-\delta}$ are given in Fig. 4 as a function of temperature in air as well as summarized in Table 1. It is worth noting that addition of iron as small as 10 mol.% in the double perovskite leads to some increase of the *Pmmm–P4/mmm* transition temperature whereas its further addition up to 20 mol.% causes obvious decrease of such temperature as seen in Fig. 4b.

The temperature of the *Pmmm–P4/mmm* phase transition was earlier confirmed [11] for $GdBaCo_{1.8}Fe_{0.2}O_{6-\delta}$ by differential scanning calorimetry (DSC). This analysis was also performed for $GdBaCo_{2-x}Fe_xO_{6-\delta}$ with $x=0.4$ and 0.6 in the present work and, as an example, its results are given for $x=0.4$ in Fig. 5. As seen DSC does not show any significant heat effects for $GdBaCo_{1.6}Fe_{0.4}O_{6-\delta}$ over complete temperature range investigated. This is the case for $GdBaCo_{1.4}Fe_{0.6}O_{6-\delta}$ as well.

It also follows from Fig. 4b that the temperature dependences of unit cell parameters of the doped double perovskite $GdBaCo_{1.4}Fe_{0.6}O_{6-\delta}$ exhibit the behavior which is quite different from that observed for the compounds with smaller content of iron. Actually this compound has the tetragonal *P4/mmm* structure at room temperature unlike $GdBaCo_{2-x}Fe_xO_{6-\delta}$ ($x=0$–0.4) and *P4/mmm-Pmmm* transition occurs at temperature as low as 170 °C while reverse transition is already observed at 290 °C in air as seen in Fig. 4b. Thus further iron addition in the double perovskite causes the dramatic change in an evolution of its structure observed with increasing temperature. For the sake of comparison the temperatures of *Pmmm-P4/mmm* transition are given in Fig. 6 for $GdBaCo_{2-x}Fe_xO_{6-\delta}$ depending on iron content. As seen this transition occurs at the same temperature for $0 \le x \le 0.1$ while the transition temperature reaches maximum for $x=0.2$ and that decreases linearly with increasing iron content.

In order to elucidate whether there is a relation between aforementioned structure transitions and oxygen content for the double perovskites studied the latter was determined in the present work as a function of temperature in air by TG method and presented in Fig. 7. Two particularities can be seen in the temperature dependences of oxygen content of the $GdBaCo_{2-x}Fe_xO_{6-\delta}$ double perovskite. First, oxygen content determined for $GdBaCo_{2-x}Fe_xO_{6-\delta}$ at a given temperature increases with increasing iron content. Second, the onset of oxygen content change shifts to lower temperature with increasing iron content (see Fig. 7 and insertion).

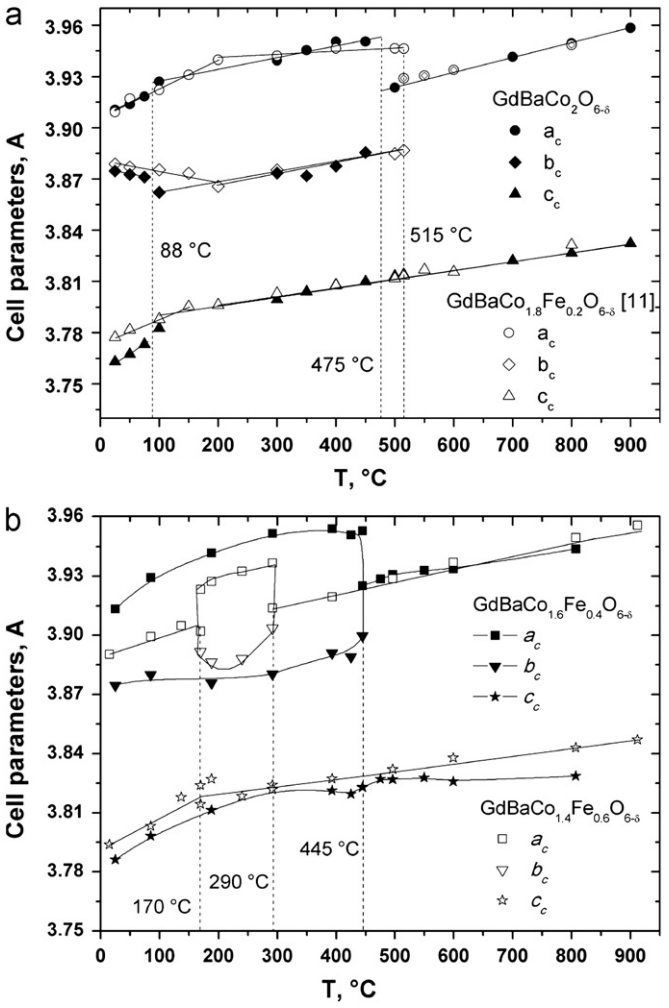

Fig. 4. Lattice parameters of $GdBaCo_{2-x}Fe_xO_{6-\delta}$ ($x=0$–0.6) vs. temperature in air. Lines are guide to eye only.

It is of interest to compare the data on oxygen content shown in Fig. 7 with those reported for $GdBaCo_{2-x}Fe_xO_{6-\delta}$ earlier by Kim et al. [9] and Kulka et al. [15]. It follows from the comparison that the data on oxygen content for the undoped $GdBaCoO_{6-\delta}$ are in good agreement whereas those differ from each other very much for the doped double perovskites $GdBaCo_{2-x}Fe_xO_{6-\delta}$. For instance, the oxygen content shown in Fig. 7 increases with iron content at a given temperature and a similar trend was observed by authors [9] whereas the contrary one was found in Ref. [15]. However, the trend on increase of oxygen content upon iron doping seems to be more physically meaningful due to increase of binding energy between adjacent oxygen and 3d-metal caused by the substitution of iron for cobalt in $GdBaCoO_{6-\delta}$. This assumption is strongly supported by the results for other double perovskites reported by authors [16] who showed that a doping $NdBaCoO_{6-\delta}$ with iron leads to oxygen content increase as well. On the other hand, the value of oxygen content as high as 5.98 determined by Kim et al. [9] for $GdBaCo_{1.5}Fe_{0.5}O_{6-\delta}$ at room temperature seems to be overestimated.

Temperature dependences of unit cell parameters (see Fig. 4) were recalculated using the data shown in Fig. 7 in oxygen content ones for the oxides studied and presented in Fig. 8. As follows the *Pmmm-P4/mmm* structure transition is observed at the same value of oxygen content equal to 5.47 for the

compositions with $x=0$ and 0.2 whereas that occurs at the value of 5.54 for $GdBaCo_{1.6}Fe_{0.4}O_{6-\delta}$. The latter is somewhat unexpected since the orthorhombic *Pmmm* structure of the double perovskites $GdBaCo_{2-x}Fe_xO_{6-\delta}$ ($x=0$; 0.2) is believed [10,11] to be provided by the oxygen vacancies ordering that is eliminated at oxygen content slightly less than 5.5. Comparison of Figs. 4b and 7 shows that both *P4/mmm-Pmmm* structure transition and reverse that are observed at the constant oxygen content equal to 5.61 for $GdBaCo_{1.4}Fe_{0.6}O_{6-\delta}$.

Aforementioned observations give an opportunity to draw a conclusion that the origin of the *Pmmm-P4/mmm* transition of $GdBaCo_{2-x}Fe_xO_{6-\delta}$ structure depends significantly on iron content. This transition is strongly related to the oxygen content for the undoped and weakly doped ($x \le 0.2$) double perovskites while there is no any evidence indicating in favor of that for the double perovskite enriched by iron.

4. Conclusions

The iron solubility limit, x, in $GdBaCo_{2-x}Fe_xO_{6-\delta}$ determined by means of X-ray diffraction was found to be close to 0.65 in air. The crystal structure changes of the double perovskites $GdBaCo_{2-x}Fe_xO_{6-\delta}$ ($x=0$–0.6) were studied by means of "in situ" X-ray diffraction in temperature range from 25 to 900 °C in air. The *Pmmm-P4/mmm* structure transition upon temperature increase was found to occur in $GdBaCo_{2-x}Fe_xO_{6-\delta}$ ($0 \le x \le 0.4$). This transition is observed at the same temperature for the compositions with $0 \le x \le 0.1$ while the transition temperature reaches maximum for the compound with $x=0.2$ and that decreases linearly with increasing iron content. The double perovskite $GdBaCo_{1.4}Fe_{0.6}O_{6-\delta}$ was shown to have the tetragonal *P4/mmm* structure at room temperature unlike $GdBaCo_{2-x}Fe_xO_{6-\delta}$ ($x=0$–0.4) and the *P4/mmm-Pmmm* structure transition occurs at temperature as low as 170 °C while

Table 1
Lattice parameters of double perovskites $GdBaCo_{2-x}Fe_xO_{6-\delta}$ ($x=0$–0.6).

Oxide	T, °C	6-δ	Space group	Cell parameters			R_{Br}	R_p
				a, Å	*b*, Å	*c*, Å		
$GdBaCo_2O_{6-\delta}$	25	5.515	*Pmmm*	3.910(6)	7.749(2)	7.526(0)	0.04	8.10
	50	5.515		3.913(8)	7.745(2)	7.534(9)	0.03	7.96
	75	5.515		3.918(3)	7.742(3)	7.546(4)	0.12	8.32
	100	5.515		3.927(0)	7.724(3)	7.565(2)	0.35	7.76
	300	5.515		3.939(4)	7.747(0)	7.599(0)	0.07	9.0
	350	5.515		3.945(5)	7.743(6)	7.608(0)	0.04	10.05
	400	5.515		3.950(5)	7.755(0)	7.616(0)	0.08	9.10
	450	5.505		3.950(5)	7.771(0)	7.620(0)	0.05	9.20
	500	5.440	*P4/mmm*	3.923(5)	3.923(5)	7.626(5)	0.04	8.50
	700	5.280		3.941(5)	3.941(5)	7.644(5)	0.07	10.31
	800	5.196		3.949(5)	3.949(5)	7.653(5)	0.03	9.30
	900	5.129		3.958(5)	3.958(5)	7.664(5)	0.1	8.50
$GdBaCo_{1.8}Fe_{0.2}O_{6-\delta}$	25	5.561	*Pmmm*	3.909(2)	7.757(6)	7.554(8)	0.02	5.18
	50	5.561		3.917(1)	7.754(0)	7.563(4)	0.02	7.69
	100	5.561		3.922(1)	7.750(8)	7.569(2)	0.02	7.80
	150	5.561		3.931(0)	7.746(6)	7.590(8)	0.04	7.22
	200	5.561		3.939(8)	7.731(3)	7.592(4)	0.02	6.10
	300	5.561		3.941(7)	7.750(5)	7.606(0)	0.02	6.02
	400	5.544		3.946(5)	7.755(0)	7.615(2)	0.03	9.0
	500	5.482		3.946(5)	7.769(4)	7.623(4)	0.02	7.63
	515	5.470		3.946(3)	7.773(7)	7.628(3)	0.04	6.83
			P4/mmm	3.929(0)	3.929(0)	7.626(8)		
	550	5.445		3.930(5)	3.930(5)	7.633(8)	0.04	7.47
	600	5.404		3.933(8)	3.933(8)	7.631(3)	0.02	8.19
	800	5.235		3.948(5)	3.948(5)	7.663(0)	0.03	7.11

Table 1 (*continued*)

$GdBaCo_{1.6}Fe_{0.4}O_{6-\delta}$	85	5.557	*Pmmm*	3.929(2)	7.760(1)	7.596(5)	0.20	11.02
	188	5.557		3.941(8)	7.751(8)	7.622(6)	0.15	10.89
	292	5.557		3.951(7)	7.761(0)	7.644(1)	0.08	14.46
	393	5.557		3.954(0)	7.782(2)	7.642(5)	0.20	10.51
	425	5.540		3.950(8)	7.778(8)	7.638(8)	0.18	10.78
	445	5.537		3.953(0)	7.799(4)	7.646(0)	0.26	13.11
			P4/mmm	3.925(2)	3.925(2)	7.645(6)		
	475	5.513		3.928(6)	3.928(6)	7.654(0)	0.07	11.69
	496	5.500		3.930(9)	3.930(9)	7.653(7)	0.11	10.00
	550	5.468		3.932(9)	3.932(9)	7.655(5)	0.09	10.52
	599	5.435		3.933(6)	3.933(6)	7.651(6)	0.08	10.37
	807	5.260		3.943(7)	3.943(7)	7.657(4)	0.12	11.20
$GdBaCo_{1.4}Fe_{0.6}O_{6-\delta}$	25	5.605	*P4/mmm*	3.890(3)	3.890(3)	7.587(6)	0.32	7.73
	85	5.605		3.899(4)	3.899(4)	7.606(4)	0.4	9.11
	137	5.605		3.904(9)	3.904(9)	7.635(8)	0.09	10.62
	170	5.605		3.902(1)	3.902(1)	7.628(6)	0.12	12.63
			Pmmm	3.923(2)	7.783(6)	7.647(8)		
	188	5.605		3.927(3)	7.772(9)	7.654(0)	0.24	8.62
	240	5.605		3.932(4)	7.776(3)	7.636(7)	0.33	6.23
	292	5.605		3.936(6)	7.807(2)	7.648(2)	0.58	20.77
			P4/mmm	3.913(9)	3.913(9)	7.643(5)		
	393	5.577		3.919(6)	3.919(6)	7.654(6)	0.07	8.02
	496	5.520		3.928(7)	3.928(7)	7.664(2)	0.08	9.23
	599	5.455		3.937(1)	3.937(1)	7.675(8)	0.09	8.48
	807	5.300		3.949(6)	3.949(6)	7.686(1)	0.05	9.68
	912	5.230		3.955(7)	3.955(7)	7.694(0)	0.06	9.75

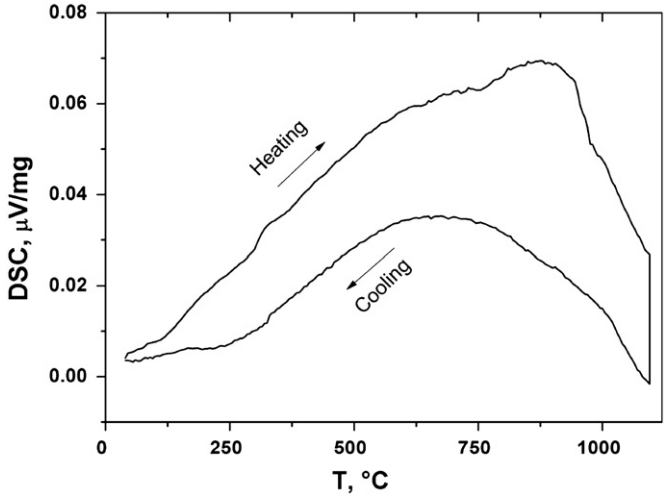

Fig. 5. DSC results for $GdBaCo_{1.6}Fe_{0.4}O_{6-\delta}$.

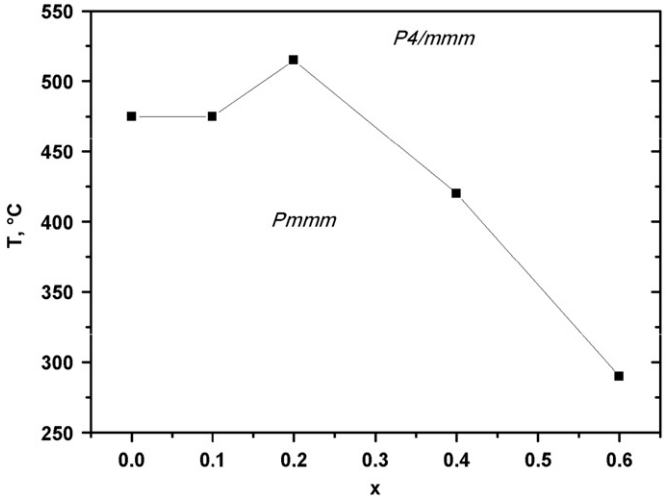

Fig. 6. *Pmmm*–*P*4/*mmm* transition temperature for $GdBaCo_{2-x}Fe_xO_{6-\delta}$ (x=0–0.6) as a function of Fe content. Lines are guide to eye only.

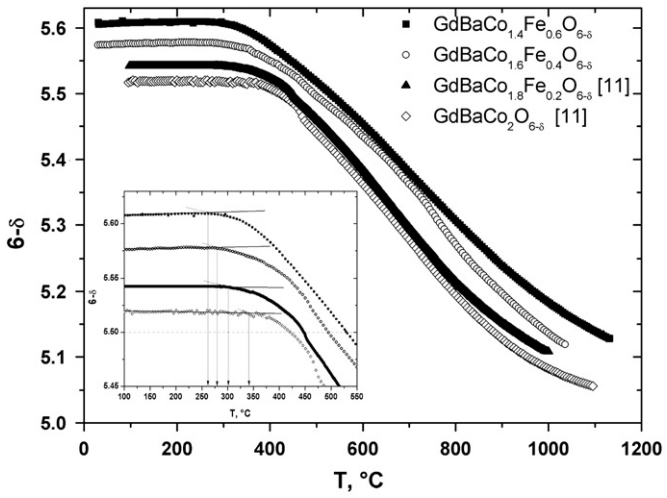

Fig. 7. Oxygen content of $GdBaCo_{2-x}Fe_xO_{6-\delta}$ ($x=0$–0.6) as a function of temperature in air.

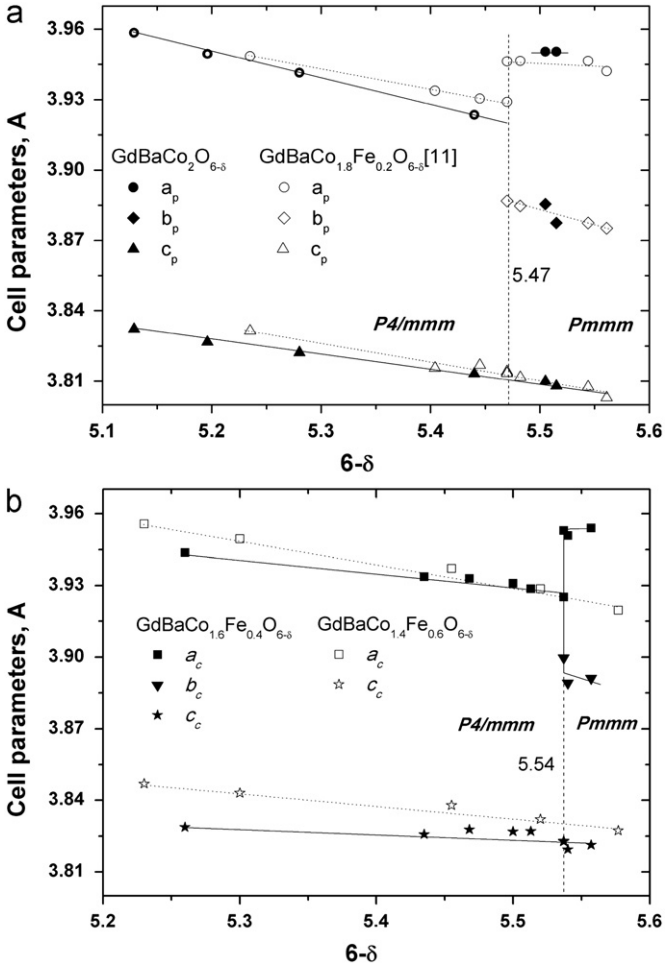

Fig. 8. Lattice parameters of double perovskites $GdBaCo_{2-x}Fe_xO_{6-\delta}$ ($x=0$–0.6) vs. oxygen content. Lines are guide to eye only.

reverse one is already observed at 290 °C in air. Oxygen content for the double perovskites studied was determined as a function of temperature in air by TG method. $GdBaCo_{2-x}Fe_xO_{6-\delta}$ oxygen content was found to increase with increasing iron content at a given temperature. The *P*4/*mmm*-*Pmmm* structure transition was shown to be strongly related to the oxygen content for the undoped and slightly doped ($x \leq 0.2$) double perovskites while there is no such evidence indicating in favor of this for the double perovskites enriched by iron.

Acknowledgments

This work was supported by the Ministry of Education and Science of the Russian Federation within the framework of Federal Program "Investigations and researches on the priority directions of development for the scientific and technological complex of Russia in 2007–2013".

References

[1] A. Maignan, C. Martin, D. Pelloquin, N. Nguyen, B. Raveau, J. Solid State Chem. 142 (1999) 7.
[2] J.C. Burley, J.F. Mitchell, S. Short, D. Miller, Y. Tang, J. Solid State Chem. 170 (2003) 339.
[3] A.A. Taskin, A.N. Lavrov, Y. Ando, Appl. Phys. Lett. 86 (2005) 091910.
[4] Lorenzo Malavasi, Yuri Diaz-Fernandez, M. Cristina Mozzati, Clemens Ritter, Solid State Commun. 148 (2008) 87.
[5] J.H. Kim, A. Manthiram, J. Electrochem. Soc. 155 (2008) B385.
[6] K. Zhang, L. Ge, R. Ran, Z. Shao, S. Liu, Acta Mater. 56 (2008) 4876.
[7] J.H. Kim, F. Prado, A. Manthirama, J. Electrochem. Soc. 155 (2008) B1023.
[8] A. Tarancón, J. Peña-Martínez, D. Marrero-López, A. Morata, J.C. Ruiz-Morales, P. Núñez, Solid State Ionics 179 (2008) 2372.
[9] Y.N. Kim, J.H. Kim, A. Manthiram, J. Power Sources 195 (2010) 6411.
[10] A. Tarancón, D. Marrero-López, J. Peña-Martínez, J.C. Ruiz-Morales, P. Núñez, Solid State Ionics 179 (2008) 611.
[11] D.S. Tsvetkov, I.L. Ivanov, A.Yu. Zuev, Solid State Ionics 218 (2012) 13.
[12] D.S. Tsvetkov, V.V. Sereda, A.Yu. Zuev, Solid State Ionics 180 (2010) 1620.
[13] D.A. Medvedev, T.A. Zhuravleva, A.A. Murashkina, V.S. Sergeeva, B.D. Antonov, Russ. J. Phys. Chem. A 84 (2010) 1623.
[14] N. Thirumurugan, A. Bharathi, C.S. Sundar, J. Magn. Magn. Mater. 322 (2010) 152.
[15] A. Kulka, Y. Hu, G. Dezanneau, J. Molenda, Funct. Mater. Lett. 4 (2011) 157.
[16] V.A. Cherepanov, T.V. Aksenova, L.Ya. Gavrilova, K.N. Mikhaleva, Solid State Ionics 188 (2011) 53.